Determination of sugar conformation in large RNA oligonucleotides from analysis of dipole–dipole cross correlated relaxation by solution NMR spectroscopy

Christian Richter[a], Christian Griesinger[a], Isabella Felli[a], Paul T. Cole[b], Gabriele Varani[b] & Harald Schwalbe[c],*

[a]*Institut für Organische Chemie, Johann-Wolfgang-Goethe-Universität Frankfurt, Marie-Curie-Straße 11, D-60439 Frankfurt/M., Germany*
[b]*Laboratory of Molecular Biology, Hills Road, Cambridge CB2 2QH, U.K.*
[c]*Massachusetts Institute of Technology, Department of Chemistry, Francis Bitter Magnet Laboratory, 170 Albany Street, Bldg. NW14, Cambridge, MA 02139, U.S.A.*

Abstract

A new experiment, the forward directed quantitative Γ-HCCH-TOCSY for the measurement of the conformation of the five-membered ribosyl unit in RNA oligonucleotides, is presented. The experiment relies on quantification of cross peak intensities caused by evolution of CH,CH-dipole–dipole cross correlated relaxation in non-evolution periods and the resolution enhancement obtainable in *forward directed* HCC-TOCSY transfer. Cross correlated relaxation rates are interpreted to reveal the sugar conformation of 22 out of 25 nucleotides in an isotopically labelled 25-mer RNA. The results obtained with this new method are in agreement with the conformational analysis derived from ^{3}J(H,H) coupling constants.

Introduction

The pseudorotation phase and amplitude (Altona and Sundaralingam, 1972) defining the conformation of the five-membered ribosyl ring in RNA and DNA oligonucleotides can be determined from interpretation of scalar ^{3}J(H,H) coupling constants (Haasnoot et al., 1980). While this is a powerful approach in small and medium size RNA isotopically labelled with ^{13}C (Schwalbe et al., 1994, 1995; Schmitz and James, 1995), scalar homonuclear ^{3}J(H,H) coupling constants in larger oligonucleotides and proteins are affected by differential relaxation of the submultiplet components (Harbison, 1993; Norwood, 1993; Conte et al., 1996; Zimmer et al., 1996). Differential relaxation affects the size of the apparent coupling constants as determined by fitting the displacement of multiplet

components (Schwalbe et al., 1993) in E.COSY experiments (Griesinger et al., 1985, 1986, 1987). 'Correct' values of coupling constants can be retrieved by simulation of individual multiplet components taking auto and cross correlated relaxation into account (Zimmer et al., 1996; Carlomagno et al., 1998). Here we introduce a method to obtain torsional angle information to determine the sugar pucker mode. The new method exploits cross correlated relaxation and thereby takes advantage of the fact that cross correlated relaxation scales linearly with the overall correlation time of a molecule. By combining the quantitative approach (Felli et al., 1999) to extract cross correlated relaxation with resolution enhancement methods using restricted coherence transfer in a so-called *forward directed* TOCSY (Schwalbe et al., 1995; Glaser et al., 1996; Marino et al., 1996), the proposed experiment could successfully be applied to a uniformly ^{13}C,^{15}N labelled 25-mer RNA and should prove to be robust

*To whom correspondence should be addressed. E-mail: schwalbe@ccnmr.mit.edu

even for large RNA oligonucleotides with anisotropic overall tumbling.

Results and discussion

Cross correlated relaxation effects of double and zero quantum coherence can be exploited to obtain structural information in proteins (Reif et al., 1997; Yang et al., 1997, 1998, 1999; Brutscher et al., 1998; Griesinger et al., 1999; Pelupessy et al., 1999), in oligonucleotides (Felli et al., 1999) and in metallo-organic compounds (Reif et al., 1998). Cross correlated relaxation rates in the 'transfer-NOE' regime have been proven to deliver the conformations of ligands weakly bound to proteins (Blommers et al., 1999; Carlomagno et al., 1999).

The dipole–dipole relaxation rate caused by cross correlated relaxation $\Gamma^c_{C_{i'}H_{i'},C_{(i+1)'}H_{(i+1)'}}$ of carbon double and zero quantum coherence (with $C_{i'}$ and $C_{(i+1)'}$ as active nuclei) is given by:

$$
\Gamma^c_{C_{i'}H_{i'},C_{(i+1)'}H_{(i+1)'}} = \frac{2}{5} \frac{\gamma_H^2 \gamma_C^2}{r^3_{C_{i'}H_{i'}} r^3_{C_{(i+1)'}H_{(i+1)'}}} \left(\frac{\mu_0}{4\pi}\right)^2
$$
$$
\hbar^2 \left(S^c_{i,(i+1)}\right)^2 j^{q,iso}_{VW}(\omega_q) \qquad (1)
$$
$$
with \; j^{q,iso}_{VW}(\omega_q) = \frac{1}{10}\{1/2(3\cos^2\theta_{VW} - 1)
$$
$$
\frac{2\tau_c}{1+(\omega_q\tau_c)^2}\}
$$

where γ_H, γ_C are the gyromagnetic ratios, μ_0 is the susceptibility of the vacuum, $r_{C_iH_i}$ and $r_{C_{(i+1)}H_{(i+1)}}$ are the carbon-proton distances, $\hbar$ is the Planck constant divided by 2π, $S^c_{i,(i+1)}$ is an order parameter taking internal mobility of the dipole tensors of $C_{i'}H_{i'}$ and $C_{(i+1)'}H_{(i+1)'}$ into account, $\theta_{i,(i+1)}$ is the projection angle between these dipole tensors, which are oriented parallel to the respective carbon-proton bond vectors, and τ_c is the overall correlation time. For anisotropic overall tumbling, the spectral density function is more complicated: For the case that $D_{xx} = D_{yy} = D_\perp$, the spectral density function of the symmetric top rotator ($D_{zz} = D_{||}$) (Schneider, 1964; Hubbard, 1969) is given by

$$
j^q_{VW}(\omega_q) = \frac{1}{20}\left\{(3\cos^2\theta_V - 1)(3\cos^2\theta_W - 1)\right.
$$
$$
\cdot J^{q,0}_{VW}
$$
$$
+ 12\cos\theta_V \cos\theta_W \sin\theta_V \sin\theta_W \cos(\phi_V
$$
$$
- \phi_W) \cdot J^{q,1}_{VW}
$$
$$
+ 3\sin^2\theta_V \sin^2\theta_W \cos(2\phi_V - 2\phi_W)
$$
$$
\left. \cdot J^{q,2}_{VW}\right\} \qquad (2)
$$

with the reduced spectral density functions ($-2 \leq m \leq +2$)

$$
J^{q,m}_{VW} = \frac{2\tau_{c,m}}{1 + (\omega_q\tau_{c,m})^2} \qquad (3)
$$

The correlation times $\tau_{c,m}$ depend on the diffusion constant $D_{||}$ along the long axis and the perpendicular diffusion constant $D_\perp$ according to

$$
1/\tau_{c,m} = 6D_\perp + m^2(D_{||} - D_\perp) \qquad (4)
$$

Here, we propose a new method called *forward directed quantitative Γ-HCCH-TOCSY*, which combines resolution enhancement via selective coherence transfer as provided in a *forward directed* HCC-TOCSY element (Schwalbe et al., 1995; Glaser et al., 1996; Marino et al., 1996) with the *quantitative Γ-HCCH* experiment (Felli et al., 1999). We demonstrate the potential of the new method by application to a 25-mer RNA, uniformly labelled with ^{13}C and ^{15}N.

The pulse sequence of the *forward directed quantitative Γ-HCCH-TOCSY* experiment is shown in Figure 1. The experiment begins with frequency labelling H1' in ω_1. A selective coherence transfer from the H1' spin is achieved by isotropic mixing in a CC-TOCSY for τ_I and longitudinal mixing for τ_L. In spin systems with uniform homonuclear ^{1}J(C,C) coupling constants, adjustment of τ_I and τ_L leads to selection of *forward directed* operators of type $2C_{i'x}C_{(i+1)'z}$ with i = 1,2,3, while operators $C_{i'x}$ and *backward directed* operators $2C_{i'x}C_{(i-1)'z}$ are suppressed (Schwalbe et al., 1995; Glaser et al., 1996; Marino et al., 1996). For τ_I = 8.9 ms and τ_L = 8.3 ms, optimal coherence transfer is observed for the operators with i = 1,2,3. After frequency labelling $C_{i'}$ in ω_2, double and zero quantum coherence $4H_{i'z}C_{i'x}C_{(i+1)'y}$ is created at the beginning of τ_M.

In the following, we summarise the discussion given in Felli et al. (1999) for the evolution of coherences $4H_{i'z}C_{i'x}C_{(i+1)'y}$ under dipole–dipole cross correlated relaxation. During the mixing time τ_M and for $\Delta' = 0$, evolution of chemical shift, of heteronuclear scalar coupling and dipole–dipole-CSA cross correlated relaxation are refocussed. Dipole–dipole cross correlated relaxation $\Gamma^c_{C_{i'}H_{i'},C_{i+1'}H_{i+1'}}$ leads to conversion of $4H_{i'z}C_{i'x}C_{(i+1)'y}$ into $4H_{(i+1)'z}C_{(i+1)'x}C_{i'y}$. The latter coherence gives rise to the cross peak at $\omega_1(H_i')$, $\omega_2(C_i')$, $\omega_3(H'_{i+1})$. Selecting this transfer allows to separate $\Gamma^c_{C_{i'}H_{i'},C_{i+1'}H_{i+1'}}$ from proton-proton H_i'-H'_{i+1} NOE which leads to $4H_{(i+1)'z}C_{i'x}C_{(i+1)'y}$. To quantitatively determine the cross correlated relaxation rate $\Gamma^c_{C_{i'}H_{i'},C_{i+1'}H_{i+1'}}$, the evolution of the original coher-
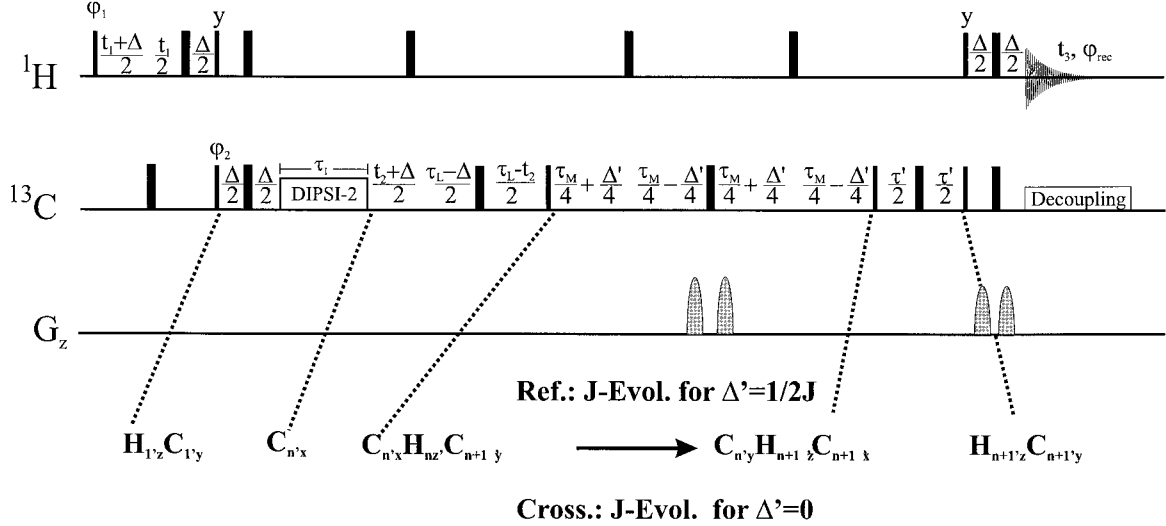
Figure 1. Pulse sequence of the 3D *forward directed quantitative* Γ-HCCH-TOCSY. Narrow and thick bars represent 90° and 180° pulses. The default phase for pulses is x. $\Delta' = 0$ ms for the cross experiment and $\Delta' = 3$ ms for the reference experiment. $\Delta = 3.2$ ms, $\tau_I = 8.9$ ms, $\tau_L = 8.3$ ms, $\tau_M = 1/(^1J_{CC}) = 25$ ms, $\tau' = 6.25$ ms. ^{13}C-decoupling was applied during acquisition with $\gamma B_1/2\pi = 2.5$ kHz. The relaxation delay was 1.5 s. The experiments were performed on a Bruker DRX600 with a ^{1}H,^{13}C,^{31}P-TXI-probe with z-gradients. Quadrature detection in ω_1 was achieved by States-TPPI phase incrementation of phase φ_1 and 8 (cross experiment: 16) scans per t_1 (64 complex points, spectral width: 1666 Hz), t_2 (48 complex points, spectral width: 5883 Hz) increments were recorded with 1K points in t_3 (spectral width: 4807 Hz). The total time was 24 h for the reference experiment and 48 h for the cross experiment (the phase cycle employed was: $\varphi_1 = x,x,-x,-x$; $\varphi_2 = x,-x$; $\varphi_{rec} = x,-x,-x,x$).

ence during the mixing time τ_M should be quantified. Evolution of the original operator under cross correlated relaxation and scalar heteronuclear coupling during τ_M is given by:

$$4H_{i'z}C_{i'x}C_{(i+1)'y} \longrightarrow$$
$$4H_{i'z}C_{i'x}C_{(i+1)'y} \left[\cosh\left(\Gamma^c_{C_iH_i,C_{(i+1)'}H_{(i+1)'}}\tau_M\right) \right.$$
$$\cos^2(\pi J_{CH}\Delta') - \sinh\left(\Gamma^c_{C_iH_i,C_{(i+1)'}H_{(i+1)'}}\tau_M\right)$$
$$\left. \sin^2(\pi J_{CH}\Delta') \right]$$
$$-4H_{(i+1)'z}C_{(i+1)'x}C_{i'y} \left[\sinh\left(\Gamma^c_{C_iH_i,C_{(i+1)'}H_{(i+1)'}}\tau_M\right) \right.$$
$$\cos^2(\pi J_{CH}\Delta') - \cosh\left(\Gamma^c_{C_iH_i,C_{(i+1)'}H_{(i+1)'}}\tau_M\right)$$
$$\left. \sin^2(\pi J_{CH}\Delta') \right] \tag{5}$$

In the experiment with $\Delta' = 0$, the intensity of the cross peak (I^{cross}) is proportional to $\sinh(\Gamma^c_{C_iH_i,C_jH_j}\tau_M)$, whereas for $\Delta' = 1/2\,J_{CH}$, the intensity of the cross peak (I^{ref}) is proportional to $\cosh(\Gamma^c_{C_iH_i,C_jH_j}\tau_M)$. By comparing the intensities of the cross peak at $\omega_1(H'_i)$, $\omega_2(C'_i)$, $\omega_3(H'_{i+1})$ in two experiments with $\Delta' = 0$ and $\Delta' = 1/2J_{CH}$, the cross correlated relaxation rate can be extracted from the intensity ratio I^{cross}/I^{ref} through the following relation:

$$\Gamma^c_{C_{i'}H_{i'},C_{i+1'}H_{i+1'}} = \frac{1}{\tau_M}\tanh^{-1}\left(\frac{I^{cross}}{I^{ref}}\right) \tag{6}$$

As can be inferred from inspection of the dependence of the rates caused by cross correlated relaxation from the pseudorotation phase (Figure 2), the relative signs of the relaxation rates provide clear evidence to discriminate between the two most prominent pseudorotation phases C3'-endo and C2'-endo: In the C3'-endo regime, $\Gamma^c_{C_{1'}H_{1'},C_{2'}H_{2'}}$ is negative and $\Gamma^c_{C_{3'}H_{3'},C_{4'}H_{4'}}$ is positive, while the opposite is true in the C2'-endo regime. This holds regardless of the correlation time τ_c and anisotropy of diffusion. The dimensionless ratio $\Gamma^c_{C_{1'}H_{1'},C_{2'}H_{2'}}/\Gamma^c_{C_{3'}H_{3'},C_{4'}H_{4'}}$ is independent of τ_c for isotropic reorientation. Therefore, analysis of the sign of the relaxation rates and their ratio provides a clear indication to assess the conformation of the ribosyl ring.

Figures 3a,b show the schematic two-dimensional planes taken at specific H1' resonances in ω_1 for the cross and reference experiment. In the cross experiment, cross peaks are expected at the resonance positions $\omega_1(H'_i)$, $\omega_2(C'_i)$, $\omega_3(H'_{i+1})$ with i = 1,2,3 in the ω_2,ω_3 plane, while additional peaks $\omega_1(H'_i)$, $\omega_2(C'_i)$, $\omega_3(H'_i)$ are observed in the reference experiment. In the reference experiment, the signs of the cross peaks are modulated by the evolution of homonuclear ^{1}J(C,C) coupling constants during the mixing time τ_M in the pulse sequence. C1' cross peaks
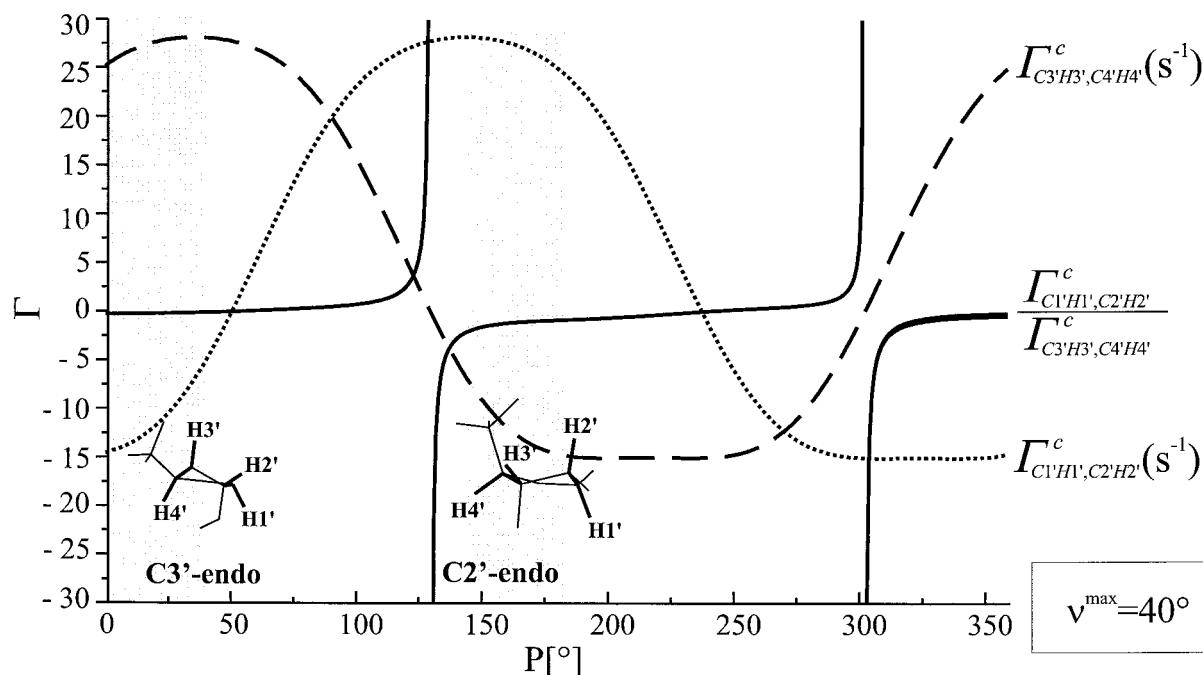
Figure 2. Relaxation rates caused by dipole–dipole cross correlated relaxation for C1′,C2′ double and zero quantum coherence and for C3′,C4′ double and zero quantum coherence, respectively, as well as their ratio are shown as a function of pseudorotation phase and a fixed pseudorotation amplitude $v^{max} = 40°$. An overall correlation time τ_c of 3.5 ns and an order parameter $S^2 = 1$ were assumed. The regions of the graph corresponding to C2′-endo and C3′-endo conformations are shaded in grey. The ratios are dimensionless, while the relaxation rates are given in s^{-1}.

have the opposite sign compared to C2′, C3′, and C4′ cross peaks. Figures 4a,b show the corresponding experimental two-dimensional planes taken at the H1′ position in ω_1 in the three-dimensional experiments. The high resolution in both reference and cross experiment is apparent. For a positive relaxation rate, cross peaks in the cross experiment have the same sign as those observed in the reference experiment. For a negative cross correlated relaxation rate, the signs are instead opposite.

The cross correlated relaxation rates have been compared with $^3J(H,H)$ coupling constants determined from *forward directed* HCC-TOCSY-CCH-E.COSY experiments (Figure 5).

The overall agreement between the two methods is good. Small $^3J(H1′,H2′)$ and large $^3J(H3′,H4′)$ coupling constants and negative $\Gamma^c_{C_{1'}H_{1'},C_{2'}H_{2'}}$ and positive $\Gamma^c_{C_{3'}H_{3'},C_{4'}H_{4'}}$ are observed for the parts of the RNA that form a regular A-form helix (see Table 1). The absolute values of the $\Gamma^c_{C_{3'}H_{3'},C_{4'}H_{4'}}$ are approximately a factor 2 larger than the $\Gamma^c_{C_{1'}H_{1'},C_{2'}H_{2'}}$, in agreement with predictions (see Figure 2). Inspection of signs of the relaxation rates clearly al-

lows to restrict the pseudorotation phase to canonical versus non-canonical conformations. We derive the pseudorotation phase from calculation of the ratio $\Gamma^c_{C_{1'}H_{1'},C_{2'}H_{2'}}/\Gamma^c_{C_{3'}H_{3'},C_{4'}H_{4'}}$, which is independent of overall correlation time and relatively insensitive to changes in the pseudorotation amplitude and internal mobility (Felli et al., 1999). For the residues in stem regions of the molecule, we find pseudorotation phase $-20° < P < 20°$, with the exception of G5, which is located at the end of stem II, and C19, which is the 3′-terminal residue; both residues undergo freighing motions (Varani et al., 1999). The values derived here suggest a rigid stem structure, the individual residues populate North-type conformations. For the loop region of the molecule, we find indication for unusual conformations from both cross correlated relaxation and coupling constants. The decreased values of $^3J(H3′,H4′)$ coupling constants and larger $^3J(H1′,H2′)$ coupling constants for residues 7 and 8 are consistent with increased $\Gamma^c_{C_{1'}H_{1'},C_{2'}H_{2'}}$ and decreased $\Gamma^c_{C_{3'}H_{3'},C_{4'}H_{4'}}$. These residues populate South-type conformations with pseudorotation phases of 149° and 148°, respectively. For averaging processes that are
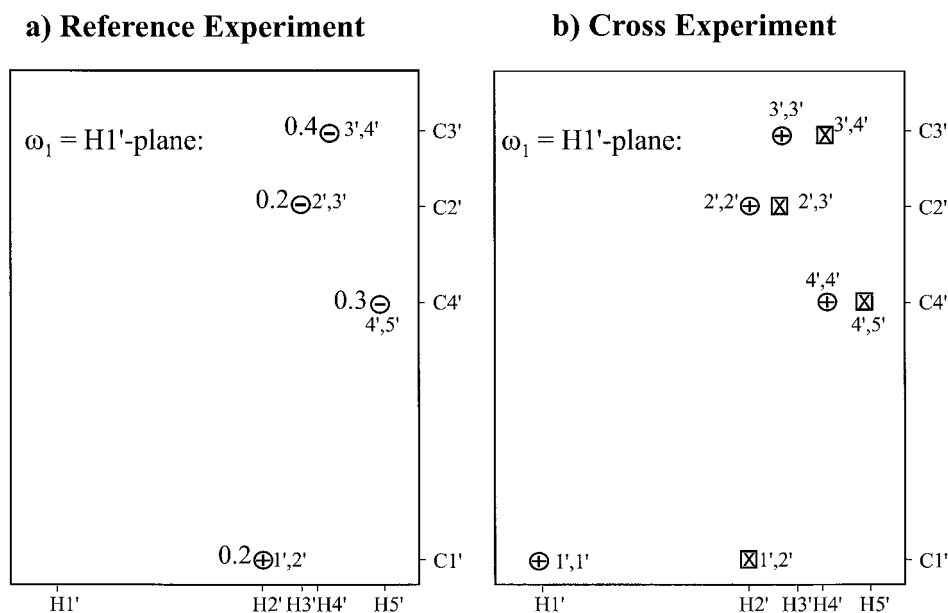
a) Reference Experiment

b) Cross Experiment

Figure 3. Schematic ^{1}H-^{13}C planes from the 3D spectra reference experiment (a) and cross experiment (b). Signs in circles indicate the sign of the cross peak in the experiments. For cross peaks indicated by squares, the sign of the cross peaks depends on the conformation. The numbers represent relative S/N.
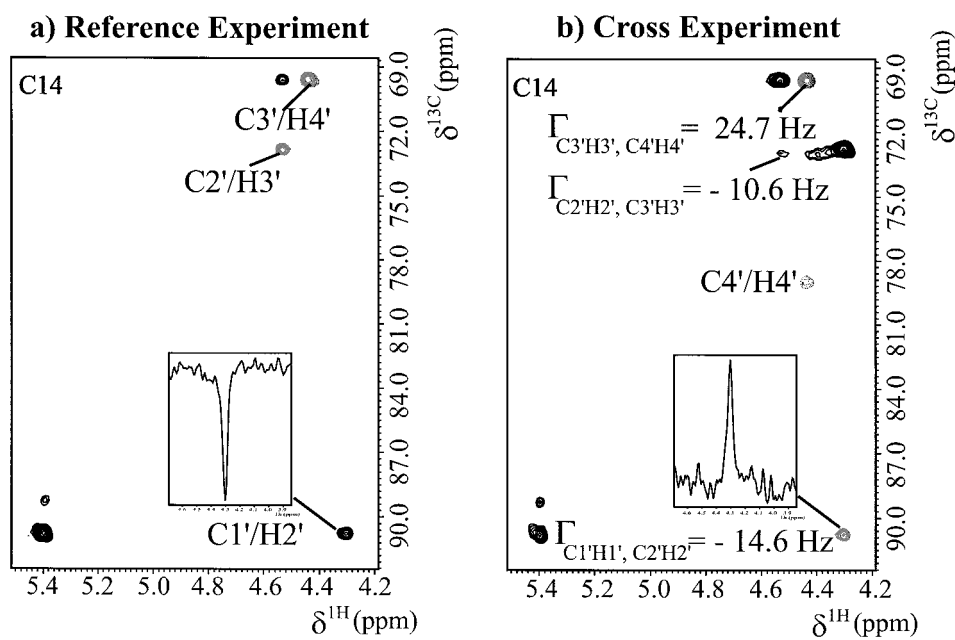
a) Reference Experiment

b) Cross Experiment

Figure 4. Experimental ^{1}H-^{13}C planes from the 3D spectra reference experiment (a) and cross experiment (b). The reference experiment was acquired in 24 h and the cross experiment was acquired in 48 h.
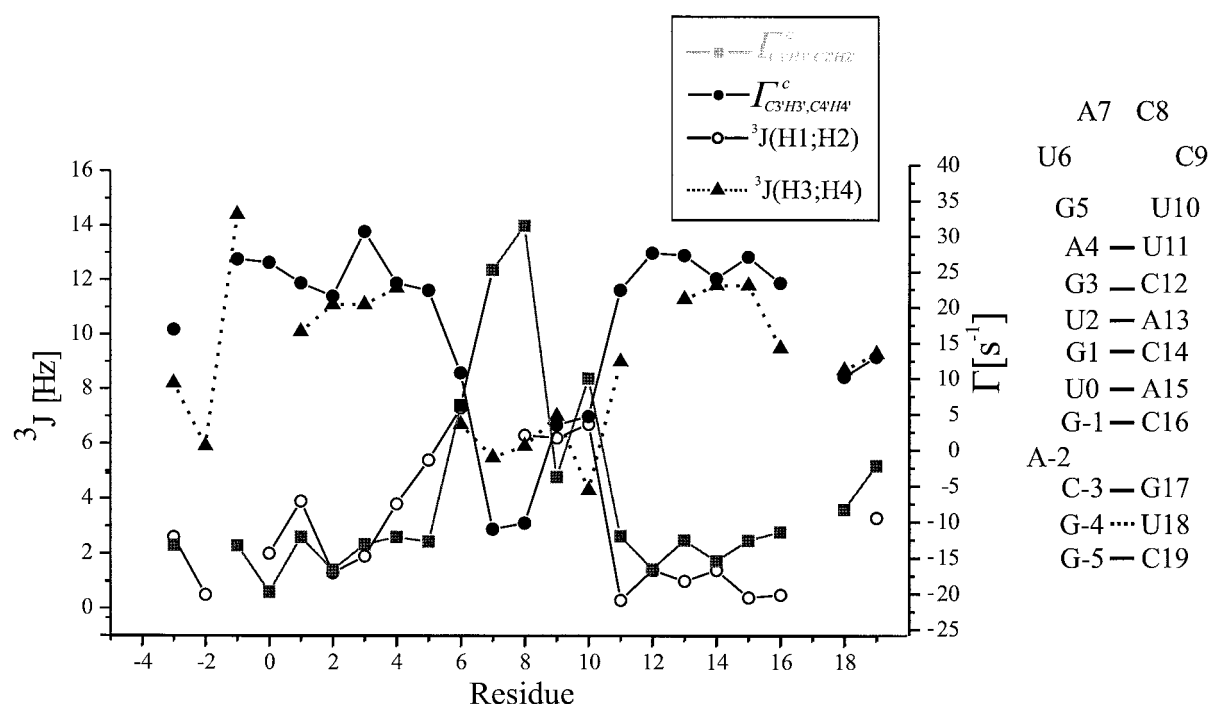
Figure 5. ^{3}J(H,H) coupling constants as determined from the HCC-TOCSY-CCH-E.COSY (Schwalbe et al., 1995) and the cross correlated relaxation rates as determined from the 3D *forward directed quantitative* Γ-HCCH-TOCSY. The secondary structure of the 25-mer RNA under investigation is shown on the right.

slow compared to the overall correlation time, the cross correlated relaxation rates are weighted by the populations of the individual conformers. For residues 6, 9 and 10, we find conformational equilibria for which North and South conformations are populated to almost equal amounts.

For isotropically tumbling molecules, the cross correlated relaxation rate scales linearly with the correlation time. In order to assess the effect of anisotropic overall tumbling, we have simulated the relaxation rates due to cross correlated relaxation for a nucleotide in a molecule tumbling anisotropically in solution. The ratio $\Gamma^c_{C_{1'}H_{1'},C_{2'}H_{2'}}/\Gamma^c_{C_{3'}H_{3'},C_{4'}H_{4'}}$ of relaxation rates caused by dipole–dipole cross correlated relaxation are found to vary depending on the orientation (θ,ϕ) of the axially symmetric diffusion tensor relative to the nucleotide. For a nucleotide with C3′-endo conformation, the ratio $\Gamma^c_{C_{1'}H_{1'},C_{2'}H_{2'}}/\Gamma^c_{C_{3'}H_{3'},C_{4'}H_{4'}}$ of -0.521 for isotropic tumbling is found to vary between -0.05 and -1.41 for an axially symmetric diffusion with $D_\perp/D_\parallel = 5$. Correcting the relaxation rates caused by cross correlated relaxation with the transverse autocorrelated relaxation rates, we obtain

a modified ratio

$$\left(\Gamma^c_{C_{1'}H_{1'},C_{2'}H_{2'}}/\Gamma^c_{C_{3'}H_{3'},C_{4'}H_{4'}}\right)\cdot\left(\Gamma^a_{C_{3'}H_{3'}}\Gamma^a_{C_{4'}H_{4'}}/\Gamma^a_{C_{1'}H_{1'}}\Gamma^a_{C_{2'}H_{2'}}\right)$$

(shown in Figure 6a) that varies between -0.2 and -0.8. For a nucleotide in C2′-endo conformation, this corrected ratio varies between -0.8 and -1.8 with a true value of -1.25. Figure 6b shows the variation of the corrected ratios also for an anisotropy of $D_\perp/D_\parallel = 10$. The calculation shows that even for a highly asymmetric molecule there are view orientations of the nucleotide relative to the main axis of the diffusion tensor that would lead to a misassignment of conformation. Furthermore, the signs of the individual rates $\Gamma^c_{C_{1'}H_{1'},C_{2'}H_{2'}}$ and $\Gamma^c_{C_{3'}H_{3'},C_{4'}H_{4'}}$ are conserved, even for anisotropic tumbling, and it is therefore still possible to distinguish the sugar pucker (C2′-endo versus C3′-endo) even for these largely anisotropic RNA oligonucleotides. It is also apparent that cross correlated relaxation of double and zero quantum coherences is more sensitive to anisotropic tumbling than auto correlated relaxation rates.

Table 2 compares the mass tensors for a number of different RNA molecules with those found for selected proteins. Both proteins and oligonucleotides possess two large mass moments and a third smaller moment.
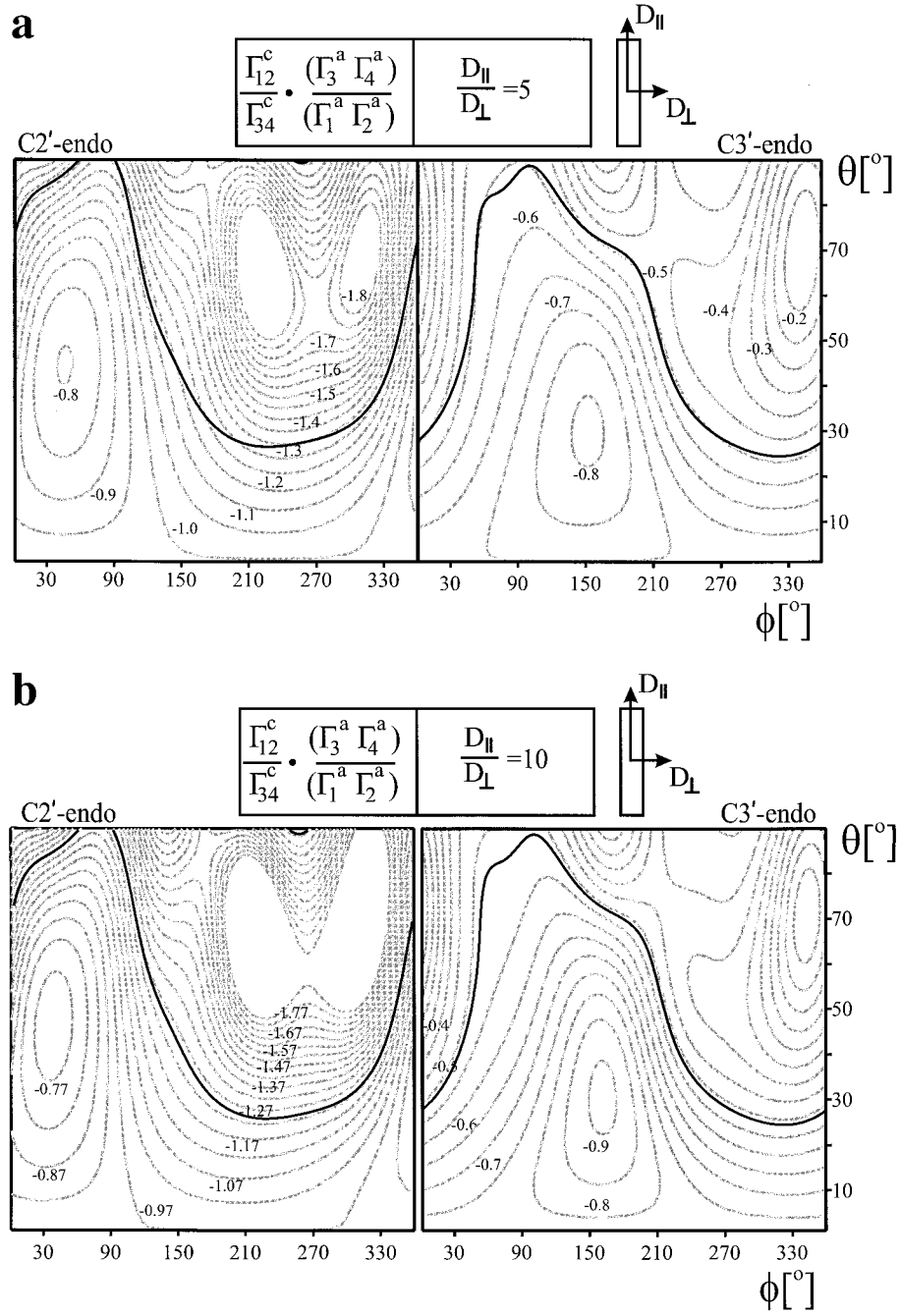
Figure 6. Variation of the ratio $\left(\Gamma^c_{C_{1'}H_{1'},C_{2'}H_{2'}} / \Gamma^c_{C_{3'}H_{3'},C_{4'}H_{4'}}\right) \cdot \left(\Gamma^a_{C_{3'}H_{3'}}, \Gamma^a_{C_{4'}H_{4'}} / \Gamma^a_{C_{1'}H_{1'}}, \Gamma^a_{C_{2'}H_{2'}}\right)$ as a function of the relative orientation of the diffusion tensor described by angles θ and ϕ and the nucleotide assuming C2′-endo or C3′-endo conformations. In (a) an anisotropy of $D_\perp/D_\| = 5$ has been assumed. In (b) an anisotropy of $D_\perp/D_\| = 10$ has been assumed. The thick and dark lines mark the ratio in absence of any anisotropy.

Table 1. Relaxation rates caused by cross correlated relaxation $\Gamma^c_{C_{i'}H_{i'},C_{(i+1)'}H_{(i+1)'}}$ (s^{-1}) as derived from the experiment shown in Figure 1 as well as proton-proton coupling constants $^3J_{H1'H2'}$ and $^3J_{H3'H4'}$ (Hz) measured from *forward directed* HCC-TOCSY-CCH-E.COSY (Schwalbe et al., 1995; Glaser et al., 1996; Marino et al., 1996) and derived pseudorotation phases (°) from cross correlated relaxation rates

	$\Gamma^c_{C1'H1',C2'H2'}$	$\Gamma^c_{C3'H3',C4'H4'}$	$\dfrac{\Gamma^c_{C1'H1',C2'H2'}}{\Gamma^c_{C3'H3',C4'H4'}}$	$^3J_{H1'H2'}$	$^3J_{H3'H4'}$	Phase
G−5	–	–	–	–	–	–
G−4	–	–	–	–	–	–
C−3	−12.5	17.6	−0.71	2.6	8.2	−15°
A−2	–	–		0.5	5.9	–
G−1	−12.5	27.4	−0.46	2.0	14.4	16°
U0	−18.9	26.9	−0.70	3.9	–	−15°
G1	−11.3	24.1	−0.47	1.3	10.1	14°
U2	−15.9	22.2	−0.71	1.9	11.1	−15°
G3	−12.3	31.3	−0.39	3.8	11.1	23°
A4	−11.3	24.1	−0.47	5.4	11.7	15°
G5	−11.9	23.0	−0.52	7.3	–	14°
U6	6.9	11.5	0.6	–	6.7	57 ± 7% 20° ; 43 ± 7% 150°
A7	24.9	> −10.2[a]	−2.4	6.3	5.5	149°
C8	32.1	−9.4	−3.4	6.2	5.9	148°
C9	−3	> 4.2[a]	−0.7	6.7	7.0	58 ± 24% 20°; 42 ± 7% 150°
U10	10.7	5.4	2.0	0.3	4.3	44 ± 1% 20°; 56 ± 7% 150°
U11	−11.2	23.1	−0.49	1.4	9.0	12°
C12	−15.8	28.2	−0.56	1.0	–	3°
A13	−11.8	27.9	−0.42	1.4	11.3	20°
C14	−14.6	24.7	−0.59	1.0	11.8	2°
A15	−11.8	27.7	−0.42	0.4	11.8	20°
C16	−10.6	24.1	−0.87	0.5	9.5	2°
G17	–	–		–	–	–
U18	−7.5	10.9	−0.68	–	8.7	−13°
C19	−1.4	13.8	−0.10	3.3	9.3	44°

[a]No cross peak observed. The given cross relaxation rates are derived from analysis of the signal-to-noise ratio in the reference experiment and extrapolating the largest relaxation rate consistent with no observation of cross peaks in the cross experiment. The pseudorotation phases were derived from the ratio of relaxation rates caused by cross correlated relaxation $\Gamma^c_{C_{1'}H_{1'},C_{2'}H_{2'}} / \Gamma^c_{C_{3'}H_{3'},C_{4'}H_{4'}}$. The error for the cross correlated relaxation rates is on the order of 1.8 s^{-1}.

The values found for RNA oligonucleotides, however, are not considerably larger than those found for proteins. An interesting comparison can be carried out between the mass tensor as calculated from the solution structure of calcium free calmodulin (Kuboniwa et al., 1995) and the anisotropic tumbling as revealed from analysis of heteronuclear relaxation rates for calcium saturated calmodulin (Barbato et al., 1992; Tjandra et al., 1996). For calmodulin, which clearly exhibits an anisotropic mass tensor (Table 2), Barbato et al. calculated a $D_\perp/D_\parallel = 2.2$–$2.7$ depending on the model assumed. In other words, even for calmodulin, with a highly asymmetric mass distribution (1.0, 0.94, 0.21), the axially symmetric diffusion tensor is only on the order of 2–3. The asymmetry of mass distribution

calculated for RNA structures in the PDB is clearly within or even smaller than what has been determined for calmodulin. Therefore, the determination of RNA conformation from cross correlated relaxation should be feasible even for larger oligonucleotides than those examined so far by NMR spectroscopy.

Conclusions

A new method is introduced that allows the determination of cross correlated relaxation rates to derive the sugar conformation in RNA oligonucleotides. The experiment is sensitive and should be valuable also for larger oligonucleotide structures than those stud-

Table 2. Relative moments of mass for selected RNA and protein structures taken from the protein data bank and calculated using the program pdbinertia[a]

Molecule	Rel. mass moments			Pdb-entry	M_r
	θ_{xx}	θ_{yy}	θ_{zz}		
RNA					
Hepatitis Delta Virus	1.0	0.93	0.20	1drz	32382
tRNA	1.0	0.80	0.33	1tra	23464
P5B stem from Tetrahymena	1.0	0.91	0.40	1ajf	5778
Tetrahymena ribozyme	1.0	0.85	0.50	1grz	153893
P4-P6 domain from Tetrahymena	1.0	0.98	0.54	1gid	98475
Proteins					
Calmodulin	1.0	0.94	0.21	1cfd	16682
Lysozyme	1.0	0.95	0.53	135l	13247

[a]Pdbinertia, written by A. Palmer (http://cpmcnet.columbia.edu/dept/gsas/biochem/labs/palmer).

ied here. The advantages of the proposed method are the following: a single line is observed for every cross peak due to the combination with resolution enhancement in the forward directed TOCSY step, and the measured effect increases with increasing molecular weight.

References

Altona, C. and Sundaralingam, M. (1972) *J. Am. Chem. Soc.*, **94**, 8205–8212.

Barbato, G., Ikura, M., Kay, L.E., Pastor, R.W. and Bax, A. (1992) *Biochemistry*, **31**, 5269–5278.

Blommers, M.J.J., Stark, W., Jones, C.E., Head, D., Owen, C.E. and Jahnke, W. (1999) *J. Am. Chem. Soc.*, **121**, 1945–1953.

Brutscher, B., Skrynnikov, N.R., Bremi, T., Brüschweiler, R. and Ernst, R.R. (1998) *J. Magn. Reson.*, **130**, 346–351.

Carlomagno, T., Schwalbe, H., Rexroth, A., Sørensen, O.W. and Griesinger, C. (1998) *J. Magn. Reson.*, **135**, 216–226.

Carlomagno, T., Felli, I.C., Czech, M., Fischer, R., Sprinzl, M. and Griesinger, C. (1999) *J. Am. Chem. Soc.*, **121**, 1945–1948.

Conte, M.R., Bauer, C.J. and Lane, A.N. (1996) *J. Biomol. NMR*, **7**, 190–206.

Felli, I.C., Richter, C., Griesinger, C. and Schwalbe, H. (1999) *J. Am. Chem. Soc.*, **121**, 1956–1957.

Glaser, S.J., Schwalbe, H., Marino, J.P. and Griesinger, C. (1996) *J. Magn. Reson.*, **B112**, 160–180.

Griesinger, C., Sørensen, O.W. and Ernst, R.R. (1985) *J. Am. Chem. Soc.*, **107**, 6394–6396.

Griesinger, C., Sørensen, O.W. and Ernst, R.R. (1986) *J. Chem. Phys.*, **85**, 6837–6852.

Griesinger, C., Sørensen, O.W. and Ernst, R.R. (1987) *J. Magn. Reson.*, **75**, 474–492.

Griesinger, C., Hennig, M., Marino, J.P., Reif, B., Richter, C. and Schwalbe, H. (1999) *Modern Methods in Protein NMR* in *Biological Magnetic Resonance Series, Vol. 16*, Plenum, London, **288**, 705–723.

Haasnoot, C.A.G., de Leeuw, F.A.A.M. and Altona, C. (1980) *Tetrahedron*, **36**, 2783–2792.

Harbison, G.S. (1993) *J. Am. Chem. Soc.*, **115**, 3026–3027.

Hubbard, P.S. (1969) *J. Chem. Phys.*, **51**, 1647.

Kuboniwa, H., Tjandra, N., Grzesiek, S., Ren, H., Klee, C.B. and Bax, A. (1995) *Nat. Struct. Biol.*, **2**, 768–776.

Marino, J.P., Schwalbe, H., Glaser, S.J. and Griesinger, C. (1996) *J. Am. Chem. Soc.*, **118**, 7251–7258.

Norwood, T.J. (1993) *J. Magn. Reson.*, **101**, 109–112.

Pelupessy, P., Chiarparin, E., Ghose, R. and Bodenhausen, G. (1999) *J. Biomol. NMR*, **13**, 375–380.

Reif, B., Hennig, M. and Griesinger, C. (1997) *Science*, **276**, 1230–34.

Reif, B., Steinhagen, H., Junker, B., Reggelin, M. and Griesinger, C. (1998) *Angew. Chem.*, **110**, 2006–2009; *Angew. Chem., Int. Ed. Engl.*, **37**, 1903–1906.

Schmitz, U. and James, T.L. (1995) *Methods Enzymol.*, **261**, 3–44, and references cited therein.

Schneider, H. (1964) *Z. Naturforsch. A*, **19**, 510.

Schwalbe, H., Marino, J.P., King, G.C., Wechselberger, R., Bermel, W. and Griesinger, C. (1994) *J. Biomol. NMR*, **4**, 631–644.

Schwalbe, H., Marino, J.P., Glaser, S.J. and Griesinger, C. (1995) *J. Am. Chem. Soc.*, **117**, 7251–7252.

Tjandra, N., Kuboniwa, H., Ren, H. and Bax, A. (1995) *Eur. J. Biochem.*, **230**, 1014–1024.

Varani, L., Hasedawa, M., Spillantini, M.G., Smith, M.J., Murrell, J.R., Ghetti, B., Klug, A., Goedert, M. and Varani, G. (1999) *Proc. Natl. Acad. Sci. USA*, **96**, 8229–8234.

Yang, D., Konrat, R. and Kay, L.E. (1997) *J. Am. Chem. Soc.*, **119**, 11938–11940.

Yang, D., Mittermaier, A., Mok, Y.-K. and Kay, L.E. (1998) *J. Mol. Biol.*, **276**, 939–954.

Yang, D., Mok, Y.-K., Muhandiram, D.R., Forman-Kay, J.D. and Kay, L.E. (1999) *J. Am. Chem. Soc.*, **121**, 3555–3556.

Zimmer, D., Marino, J.P. and Griesinger, C. (1996) *Magn. Reson. Chem.*, **34**, 177–186.